CrossMark

ORIGINAL CONTRIBUTION

Nitroglycerin induces DNA damage and vascular cell death in the setting of nitrate tolerance

Yuliya Mikhed[1] · Jörg Fahrer[2] · Matthias Oelze[1] · Swenja Kröller-Schön[1] ·
Sebastian Steven[1] · Philipp Welschof[1] · Elena Zinßius[1] · Paul Stamm[1] ·
Fatemeh Kashani[1] · Siyer Roohani[1] · Joana Melanie Kress[2] · Elisabeth Ullmann[1] ·
Lan P. Tran[1] · Eberhard Schulz[1] · Bernd Epe[3] · Bernd Kaina[2] · Thomas Münzel[1,4] ·
Andreas Daiber[1,4]

Abstract Nitroglycerin (GTN) and other organic nitrates are widely used vasodilators. Their side effects are development of nitrate tolerance and endothelial dysfunction. Given the potential of GTN to induce nitro-oxidative stress, we investigated the interaction between nitro-oxidative DNA damage and vascular dysfunction in experimental nitrate tolerance. Cultured endothelial hybridoma cells (EA.hy 926) and Wistar rats were treated with GTN (ex vivo: 10–1000 μM; in vivo: 10, 20 and 50 mg/kg/day for 3 days, s.c.). The level of DNA strand breaks, 8-oxoguanine and O^6-methylguanine DNA adducts was determined by Comet assay, dot blot and immunohistochemistry. Vascular function was determined by isometric tension recording. DNA adducts and strand breaks were induced by GTN in cells in vitro in a concentration-dependent manner. GTN in vivo administration leads to endothelial dysfunction, nitrate tolerance, aortic and cardiac oxidative stress, formation of DNA adducts, stabilization of p53 and apoptotic death of vascular cells in a dose-dependent fashion. Mice lacking O^6-methylguanine-DNA methyltransferase displayed more vascular O^6-methylguanine adducts and oxidative stress under GTN therapy than wild-type mice. Although we were not able to prove a causal role of DNA damage in the etiology of nitrate tolerance, the finding of GTN-induced DNA damage such as the mutagenic and toxic adduct O^6-methyl-guanine, and cell death supports the notion that GTN based therapy may provoke adverse side effects, including endothelial function. Further studies are warranted to clarify whether GTN pro-apoptotic effects are related to an impaired recovery of patients upon myocardial infarction.

Y. Mikhed, J. Fahrer and M. Oelze contributed equally to this work and are joint first authors.

Electronic supplementary material The online version of this article (doi:10.1007/s00395-016-0571-4) contains supplementary material, which is available to authorized users.

✉ Andreas Daiber
daiber@uni-mainz.de

1   Center of Cardiology-Cardiology 1, Molecular Cardiology, University Medical Center of the Johannes Gutenberg University, Langenbeckstr. 1, 55101 Mainz, Germany

2   Department of Toxicology, University Medical Center of the Johannes Gutenberg University, Obere Zahlbacher Str. 67, 55131 Mainz, Germany

3   Institute of Pharmacy and Biochemistry, Johannes Gutenberg University, Staudinger Weg 5, 55128 Mainz, Germany

4   German Center for Cardiovascular Research (DZHK), Partner Site Rhine-Main, Langenbeckstr. 1, 55101 Mainz, Germany

Abbreviations

ACh	Acetylcholine
t-BOOH	Tert-butyl hydroperoxide
DEA/NO	Diethylamine NONOate
DHE	Dihydroethidium
EPR	Electron paramagnetic resonance spectroscopy
eNOS	Endothelial ˙NO synthase (type 3)
ECL	Enhanced chemiluminescence
EtOH	Ethanol
GTN	Glyceryl trinitrate (nitroglycerin)
IHC	Immuno-histochemistry
ISMN	Isosorbide-5-mononitrate

🖄 Springer

L-012	8-Amino-5-chloro-7-phenylpyrido[3,4-d]pyridazine-1,4-(2H,3H)dione sodium salt
MGMT	O^6-methylguanine-DNA methyltransferase
$^\cdot$NO	Nitric oxide
Hb-NO	Nitrosyl-iron hemoglobin
3NT	3-Nitrotyrosine
O^6-me-G	O^6-methylguanine
8-oxo-G	8-Oxoguanine
RONS	Reactive oxygen and nitrogen species
SDS-Page	Sodium dodecyl sulfate-polyacrylamide electrophoresis
$O_2^{\cdot -}$	Superoxide anion radical

Introduction

Organic nitrates are still among the most commonly pre-scribed medications for the treatment of angina pectoris and myocardial infarction [19, 43]. Their beneficial anti-ischemic effects are based on endothelium-independent vasodilation of coronary arteries, venous capacity vessels and collaterals [39]. Under chronic therapy, the efficacy of organic nitrate therapy is seriously impaired by the devel-opment of pseudotolerance, due to an increase in cate-cholamines and activation of the renin–angiotensin–aldosterone system, true vascular tolerance and endothelial dysfunction accompanied by increased oxidative stress [31, 38, 39]. Our previous studies identified oxidative stress as a hallmark of nitrate tolerance and nitrate-associated endothelial dysfunction [42, 47, 58]. Sources of nitrate-induced reactive oxygen and nitrogen species formation are the mitochondrial respiratory chain complexes [8, 13], activation of the phagocytic NADPH oxidase [42, 60] and uncoupling of the endothelial nitric oxide synthase (eNOS) [31, 40].

Besides oxidative stress, organic nitrate therapy also leads to nitrosative stress [27] and both conditions favor the alkylation and oxidation of DNA bases [18]. DNA dam-aging properties were attributed not only to the organic nitrates, but also to other nitric oxide ($^\cdot$NO) releasing compounds such as diazeniumdiolates [34]. Andreassi and coworkers reported on a significant increase in DNA damage in patients under chronic organic nitrate therapy [1]. This observation does not only raise the question of whether organic nitrate-induced DNA damage contributes to the pathogenesis of nitrate tolerance, but also warrants caution for their long-term use since mutagenic DNA lesions may contribute to the development of cancer, as observed with other NO donors [18], or increased rates of cell death by apoptosis [29].

In the present study, we, therefore, investigated the effect of nitroglycerin (GTN) on cultured immortal hybri-doma cells that shares some key features with human endothelial cells (EA.hy 926) in vitro and also in vivo following GTN administration in Wistar rats with special emphasis on DNA damage induction. In order to answer the question whether the highly mutagenic and toxic DNA lesion O^6-methylguanine (O^6-me-G) contributes to the severity of nitrate tolerance and associated side effects, we studied the effect of GTN in O^6-methylguanine-DNA methyltransferase (MGMT) knockout mice deficient in the repair of O^6-me-G adducts.

Materials and methods

Materials

GTN was used either from a nitrolingual infusion solution (1 mg/ml) from G. Pohl-Boskamp (Hohenlockstedt, Ger-many) for isometric tension studies, or as an ethanol solution (100 g/l) from Novasep (Leverkusen, Germany) for induction of nitrate tolerance. L-012 (8-amino-5-chloro-7-phenylpyrido[3,4-d]pyridazine-1,4-(2H,3H)dione sodium salt) was from Wako Pure Chemical Industries (Osaka, Japan). The Bradford reagent was obtained from BioRad, Munich, Germany. ISMN was purchased from Acros Organics (Fairlawn, NJ, USA). DEA/NO was from Cayman Chemicals (Ann Arbor, MI, USA). All other chemicals were of analytical grade and were obtained from Merck, Fluka or Sigma-Aldrich.

Animals and treatment protocol

All animal treatments were in accordance with the Guide for the Care and Use of Laboratory Animals as adopted and promulgated by the U.S. National Institutes of Health and approved by the Ethics Commission according to the German Law on the Protection of Animals (Landesunter-suchungsamt Rheinland-Pfalz, Koblenz, Germany: #23 177-07/G12-1-084). In total, 68 male Wistar rats (6 weeks old, 300 g, Charles River Laboratories, Sulzfeld, Germany) were studied. Nitrate tolerance in Wistar rats was induced by twice daily subcutaneous injection of ethanolic nitro-glycerin solution (50 mg/kg/day—high dose) or by sub-cutaneously implanted osmotic pumps (Alzet model 2001, CA, USA) and infusion of GTN with doses of 10 mg/kg/day (low dose) and 20 mg/kg/day (medium dose) for 3.5 days [31]. Ethanol injections (similar volume as for the ethanolic GTN solution) served as a solvent control. MGMT$^{-/-}$ knockout mice on a C57BL/6 background [22] and C57BL/6 mice as corresponding wild-type controls were also used in this study. MGMT$^{-/-}$ knockout mice [22] were kindly provided by Leona Samson (MIT Bio-logical Engineering, Cambridge, MA, USA). A total number of 50 MGMT$^{-/-}$ knockout and age matching

C57BL/6 mice (12–14 weeks old, ~ 30 g) were treated with subcutaneous injection of ethanolic nitroglycerin solution (30 mg/kg/day) or ethanol injections for 3.5 days. Dissection of the thoracic and abdominal aorta, blood and heart was done under isoflurane anesthesia.

Isometric tension studies

Vasodilator responses to the endothelium-dependent vasodilator acetylcholine (ACh) and the endothelium-independent vasodilator GTN were assessed with endothelium-intact isolated rat and mouse aortic rings (thoracic aorta, 4 mm in length) mounted for isometric tension recordings in organ chambers as it was previously described [7, 53]. Rat aortic rings were pre-constricted by phenylephrine, mouse aortic rings were pre-constricted by prostaglandin $F_{2\alpha}$.

Detection of oxidative and nitrosative stress in whole blood, heart and aorta

Leukocyte-dependent RONS formation was measured in fresh citrate blood upon stimulation with zymosan A (50 µg/ml) in PBS buffer containing Ca/Mg (1 mM) by L-012 (100 µM) enhanced chemiluminescence (ECL) [32]. Vascular RONS formation was determined using dihydroethidium (DHE, 1 µM)-dependent fluorescence microphotography in aortic cryosections as described [40]. RONS-derived red fluorescence was detected using a Zeiss Axiovert 40 CFL microscope, Zeiss lenses and Axiocam MRm camera. Intensity of the DHE fluorescence products was evaluated by densitometry. Detection of RONS in isolated cardiac mitochondria was performed as previously described [6]. For the immuno-histochemical (IHC) analysis of 3-nitrotyrosine (3-NT) as a direct product of peroxynitrite induced nitrosative stress, aortic segments were fixed in paraformaldehyde (4 %), paraffin-embedded and stained with mouse monoclonal 3-nitrotyrosine antibody (Upstate Biotechnology, MA, USA) at a dilution of 1:100; anti-mouse biotinylated secondary antibody (1:1000) was used following the manufacturer's instructions. For immuno-chemical detection, ABC reagent (Vector) and then DAB (peroxidase substrate Kit, Vector) reagent were used as substrates. Evaluation of the immuno-histochemical results was done with the ImageJ software (NIH, USA). ˙NO bioavailability in whole blood was measured using EPR spectroscopy by nitrosyl-iron hemoglobin (Hb-NO) [46]. ˙NO bioavailability in whole blood was measured using electron paramagnetic resonance (EPR) spectroscopy by nitrosyl-iron hemoglobin (Hb-NO). Samples of venous blood were obtained by cardiac puncture of anesthetized rats; blood samples were snap frozen and later on stored in liquid nitrogen [46]. The EPR measurements were carried out at 77 K using an X-band table-top spectrometer MS400 (Magnettech, Berlin, Germany). The instrument settings were as follows: 10 mW microwave power, 7000 mG amplitude modulation, 100 kHz modulation frequency, 3300 G center field, 300 G sweep width, 60 s sweep time and 5 scans.

Western blot analysis in homogenates of EA.hy 926 cells and cardiac tissue

Lysis of EA.hy 926 cells was performed in RIPA Buffer (50 mM Tris–HCl, pH 8; 150 mM NaCl, 1 mM EDTA, 1 % NP-40, 0.5 % sodium desoxycholate, 0.1 % SDS; 1 mM PMSF, 2 mM Na_3VO_4, 1× Proteinase Inhibitor and 1 mM DTT) and protein concentration was determined by Bradford assay. Proteins were then separated by SDS-PAGE and blotted onto nitrocellulose membranes. After blocking, the membranes were incubated with the following primary antibodies: mouse monoclonal α-Hsp90 (90 kDa, 1:1000, Santa Cruz Biotechnology) as a control for loading and transfer, rabbit monoclonal α-phospho-H2AX (Ser139) (15 kDa, 1:1000, Abcam) and mouse monoclonal p53 (clone DO-I; 53 kDa, 1:500, Santa Cruz Biotechnology). Detection and quantification were performed using the Odyssey imaging system (LI-COR) with donkey anti-rabbit green (IRDye 800CW, LI-COR) or donkey anti-rabbit red (IRDye 680RD, LI-COR) and donkey anti-mouse green (IRDye 800CW, LI-COR) or donkey anti-mouse red (IRDye 680RD, LI-COR) secondary antibodies. Densitometric quantification of protein bands was performed with ImageJ 1.48v (National Institutes of Health, USA). Analysis of p53 and γ-H2AX in rat aortic tissue homogenates was performed as described previously [14].

Isolated cardiac tissue was frozen and homogenized in liquid nitrogen. Proteins were separated by SDS-Page and blotted onto nitrocellulose membranes. After blocking, immuno-blotting was performed with the following primary antibodies: polyclonal rabbit β-actin (42 kDa, 1:2500, Sigma, USA) as a control for loading and transfer, polyclonal rabbit fractin (1:1000, Millipore, Germany), polyclonal rabbit caspase-3 (1:1000, Cell Signaling, USA). Detection and quantification were performed by ECL with peroxidase conjugated anti-rabbit (1:10,000, Vector Lab., Burlingame, CA, USA) secondary antibody. Densitometric quantification of antibody-specific bands was performed with a ChemiLux Imager (CsX-1400 M, Intas, Göttingen, Germany) and Gel-Pro Analyzer software (Media Cybernetics, Bethesda, MD, USA).

Cell culture

The cultured immortal hybridoma cell line EA.hy 926 that shares some key features with human endothelial cells was a kind gift from Edgell (University of North Carolina at Chapel Hill, USA) [12]. EA.hy 926 cells were grown at 10 % CO_2 in Dulbecco's modified Eagle's medium (DMEM, Sigma) with 10 % fetal calf serum, 2 mM L-glutamine, 100 IU/ml penicillin, 100 µg/ml streptomycin and 1 mM sodium pyruvate. For experiments, the cells were seeded in 6-well plates at a density of 1.5×10^5 cells/well and grown to 60–70 % confluence.

Comet assay

As a positive control, the DNA strand breaks generator tert-butyl hydroperoxide (t-BOOH) was used. After two thorough washes with PBS buffer cells were trypsinized, resuspended in 0.5 % low melting point-agarose followed by embedding onto an agarose-pre-coated slide. As a next step, slides were incubated in lysis buffer containing 1 % sodium lauryl sarcosinate, 10 mM Tris, pH10, 2.5 M NaCl, 100 mM EDTA for 45 min followed by an unwinding step in electrophoresis buffer consisting of 1 mM EDTA pH13 and 300 mM NaOH for 20 min at 4 °C. Electrophoresis was conducted at 25 V and 300 mA for 15 min. Afterwards samples were neutralized three times with 0.4 M Tris pH 7.5 and fixed in 100 % ethanol, air-dried and stained with 50 µg/ml propidium iodide. Results were microscopically analyzed by Olympus BX50 equipped with a ColorView camera (Olympus, Münster, Germany) [15]. As an output, 50 cells were scored using Comet IV software (Perceptive Instruments Ltd., Bury St Edmunds, UK) for each sample. The Fpg-modified alkaline comet assay was conducted as previously described for the alkaline comet assay with several modifications. When the cell lysis was finished, slides were incubated in a buffer containing Fpg (1 µg/ml), 0.5 mM EDTA pH 8.0, 0.1 M KCl, 40 mM HEPES and 0.2 mg/ml BSA for 37 min at 37 °C. Next the DNA unwinding step was performed as described above [11]. The Comet assay was performed in a non-blinded fashion.

DNA extraction from the EA.hy 926 cells, aortic and cardiac tissue

Depending on the source, either cell culture or animal tissue, two different protocols for DNA extraction by phenol:chloroform:isoamyl alcohol were used. EA.hy 926 cells were washed at room temperature with PBS buffer, followed by trypsin digestion. After centrifugation at 4000g for 5 min, the cell pellet was re-suspended in the lysis buffer (100 mM NaCl, 10 mM Tris pH 8.0, 10 mM EDTA pH 8.0, 0.5 % SDS, 20 mg/ml proteinase K) and incubated overnight at 56 °C. Samples were then subjected to two rounds of phenol:chloroform:isoamyl alcohol (25:24:1) extraction followed by a chloroform washing step. Each extraction step was finished with centrifugation at 12,000g for 5 min at room temperature. The extraction procedure was finalized by DNA precipitation with one volume of sodium acetate (3 M) and three volumes of ice-cold isopropanol, and then RNA digest was applied. For this purpose, the precipitate was dissolved in TE buffer (10 mM Tris, pH8.0, 1 mM EDTA, pH8.0) and digested with RNase A/T1 mix (80 µg/ml RNase A, 200 U/ml RNase T1) for 2 h at 37 °C. Next, the solution was subjected to the 2nd procedure of phenol:chloroform:isoamyl alcohol extraction and DNA precipitation. Finally, DNA was re-suspended in TE buffer and its concentration was determined with NanoDrop 2000 UV–Vis spectrophotometer (ThermoFisher Scientific, Wilmington, USA). In the case of tissue samples, the aortas and hearts were snap frozen in liquid nitrogen immediately after the dissection and then homogenized with a pestle in a mortar in the presence of liquid nitrogen. In order to achieve a complete tissue digest, extraction buffer (0.1 M NaCl, 20 mM Tris pH8.0, 25 mM EDTA pH8.0, 0.5 % SDS, 20 mg/ml proteinase K) was added to the pulverized samples. Subsequently, DNA extraction protocol was performed as for EA.hy 926 experimental set-up.

Immuno-dot blot analysis of 8-oxoG and O^6-meG adducts in genomic DNA from EA.hy 926 cells, aortic and cardiac tissue

To detect and quantify levels of the DNA damage, we developed a new immuno-dot blot method based on the previous work of Nehls and colleagues [45]. Initially, genomic DNA was denatured at 95 °C for 5 min and mixed with an equal volume of 2 M ammonium acetate solution. Afterwards, the sample was transferred to the nitrocellulose membrane, previously equilibrated with 1 M ammonium acetate. To enhance DNA binding, the membrane was incubated in 5× SSC buffer (0.75 M NaCl, 0.075 M tri-sodium citrate). For final fixation, the membrane was kept on the heat block for 2 h at 80 °C. 0.5 % casein in PBS-T solution (0.1 % Tween 20) was used as a blocking buffer for 2 h at room temperature. Subsequently, appropriate primary antibodies were applied: monoclonal mouse anti-O^6-methyl-2-deoxyguanosine (1:500, Squarix, Marl, Germany) and monoclonal mouse anti-8-hydroxy-guanosine, clone 15A3 (1:4,000, Abcam, UK). PBS-T/NaCl solution (0.1 % Tween 20, 0.16 M NaCl) was used as a washing buffer. Next, incubation with the peroxidase conjugated anti-mouse (1:10,000, Vector Lab., Burlingame, CA, USA) secondary antibody was performed

followed by chemiluminescence detection using ECL reagent (ThermoFischer scientific, Wilmington, USA). Densitometric quantification was performed with a ChemiLux Imager (CsX-1400 M, Intas, Göttingen, Germany) and Gel-Pro Analyzer software (Media Cybernetics, Bethesda, MD, USA).

Immunohistochemical analysis of 8-oxo-G lesions and O^6-me-G adducts in aortic tissue

Immunohistochemical analysis of the aortic tissue for the presence of the oxidative DNA modifications and adducts was done as described above for the 3NT modification. The same primary antibodies as in the section "Immuno-dot blot analysis with DNA from EA.hy 926 cells, aortic and cardiac tissue" were used with a modification in the dilution range for the O^6-methyl-2-deoxyguanosine antibody (1:250). All other details were previously reported [52].

Cell death detection assay

Previously described paraffin-embedded aortic sections were de-paraffinated, rehydrated and treated with proteinase K (20 μg/ml in 10 mM Tris, pH8.0) for 30 min at 37 °C. In the subsequent steps, the tissue was permeabilized with 0.1 M citrate buffer, pH 6.0 for 20 min at 80 °C in humidified chambers. TUNEL reaction mixture was applied to the tissue according to the manufacturer's instructions (In Situ Cell Death Detection Kit, Roche, Switzerland) for 60 min at 37 °C in the humidified chamber. After several washing steps, slides were covered with the mounting medium and cover slips for the microscopic evaluation. Fluorescence was detected using a Zeiss Axiovert 40 CFL microscope, Zeiss lenses and Axiocam MRm camera. Intensity of the fluorescence products was evaluated by densitometry with the help of Gel-Pro Analyzer software (Media Cybernetics, Bethesda, MD, USA).

Statistical analysis

Data are presented as the mean value $\pm$ SEM. Two-way ANOVA (with Bonferroni's correction for comparison of multiple means) was used for comparisons of vasodilator potency and efficacy results of the isometric tension studies. 1-way ANOVA, Kruskal–Wallis 1-way ANOVA on Ranks (with Bonferroni's or Dunn's correction, or Tukey's test for comparison of multiple means) was used for the evaluation of mitochondrial RONS data, comet assay without Fpg, immuno-histochemical measurement of the O^6-me-G, 8-oxo-G and 3NT levels, protein expression analysis in tissue and DHE staining in the tissues of rats and mice. Mann–Whitney Rank Sum test was used for the evaluation of the comet assay results with the Fpg enzyme,

oxidative burst measurement in whole blood from rats or mice. t test was applied for the evaluation of the Hb-NO EPR data of rat whole blood and protein expression analysis in cell lysates.

Results

DNA damage induction in cultured EA.hy 926 cells upon GTN treatment

First, we determined GTN-induced DNA damage in cultured EA.hy 926 cells, in particular 8-oxo-G and O^6-me-G, using an immunological dot blot assay. There was a concentration-dependent increase in both DNA modifications, which became significant with a GTN concentration of 50 or 250 μM (Fig. 1a). The induction of DNA strand breaks by GTN was confirmed by the comet assay performed with or without Fpg enzyme, which removes 8-oxo-G, thereby leaving a DNA single strand break at the adduct site (Fig. 1b, c). The enhanced level of DNA strand breaks after incubation with Fpg (compared without Fpg) indicates the induction of the 8-oxo-G adducts in the DNA by GTN treatment, which is in line with the findings obtained by the dot blot analysis (Fig. 1b). Incubation of EA.hy 926 cells with GTN revealed stabilization of p53 and increased γH2AX levels at intermediate GTN concentrations (<10 μM), which was lost at higher concentrations (>10 μM) (suppl. Fig. S1). Another organic nitrate (ISMN) and the spontaneous NO donor DEA/NO showed concentration-dependent increase in DNA strand breaks in EA.hy 926 cells, without affecting p53 protein levels (suppl. Fig. S2).

Vascular activity in rat aortas

Nitrosyl-iron hemoglobin (Hb-NO) levels in whole blood can be used to measure ˙NO bioavailability and inducible ˙NO synthase activity in the circulation as previously shown for sepsis [55]. With the help of EPR spectroscopy we showed a significant increase in Hb-NO in the GTN (high dose) treated animals (suppl. Fig. S3) suggesting nitrosative stress conditions that could induce DNA damage. GTN treatment at all doses resulted in an impaired aortic response to either acetylcholine (ACh) or GTN, confirming the development of endothelial dysfunction and nitrate tolerance in the animals (Fig. 2a, b).

Nitro-oxidative stress parameters

Likewise, vascular RONS formation as measured by DHE staining showed a GTN dose-dependent increase (Fig. 2c). Levels of cardiac RONS were elevated in a GTN dose-
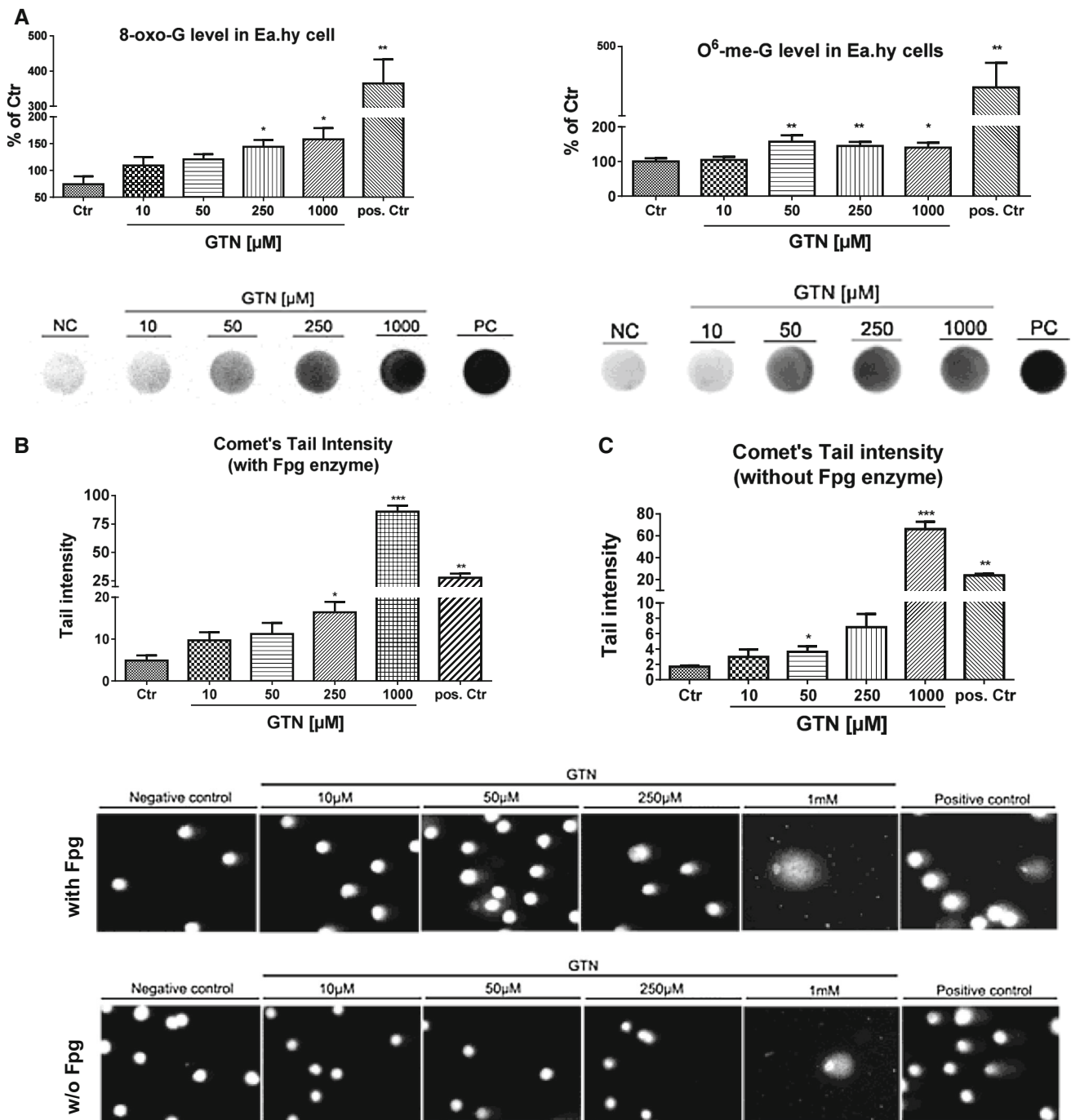
Fig. 1 DNA damage induced by GTN administration to EA.hy 926 cells. **a** Immuno-dot blot analysis for 8-oxo-G and O^6-me-G in EA.hy 926 cells that were treated for 48 h with increasing concentrations of GTN (10–1000 μM). Representative blots are shown below the densitometric quantification. **b** Read-out of alkaline comet assay with Fpg enzyme for the measurement of 8-oxo-G dependent DNA strand breaks. **c** Results of the alkaline comet assay without Fpg for the detection of natural DNA strand breaks. Representative images are shown below the densitometric quantification. Positive controls were Fenton reaction (FeSO$_4$ 100 μM, H$_2$O$_2$ 1 mM) for 8-oxo-G and MNU (500 μM) for O^6-me-G, t-BOOH (10 μM) was used as a positive control for Comet assay. The data are presented as mean value ± SEM of **a** 4; **b** 3–4; **c** 3–4 experiments. *$p < 0.05$ vs. control, **$p < 0.01$ vs control, ***$p < 0.001$ vs control

dependent fashion (Fig. 2d). Also RONS formation in zymosan A-stimulated whole blood was increased in a GTN dose-dependent manner (Fig. 2e). The nitration of protein tyrosine residues by GTN therapy was confirmed by immunohistochemical detection of 3NT-positive proteins in the rat aorta (suppl. Fig. S4).
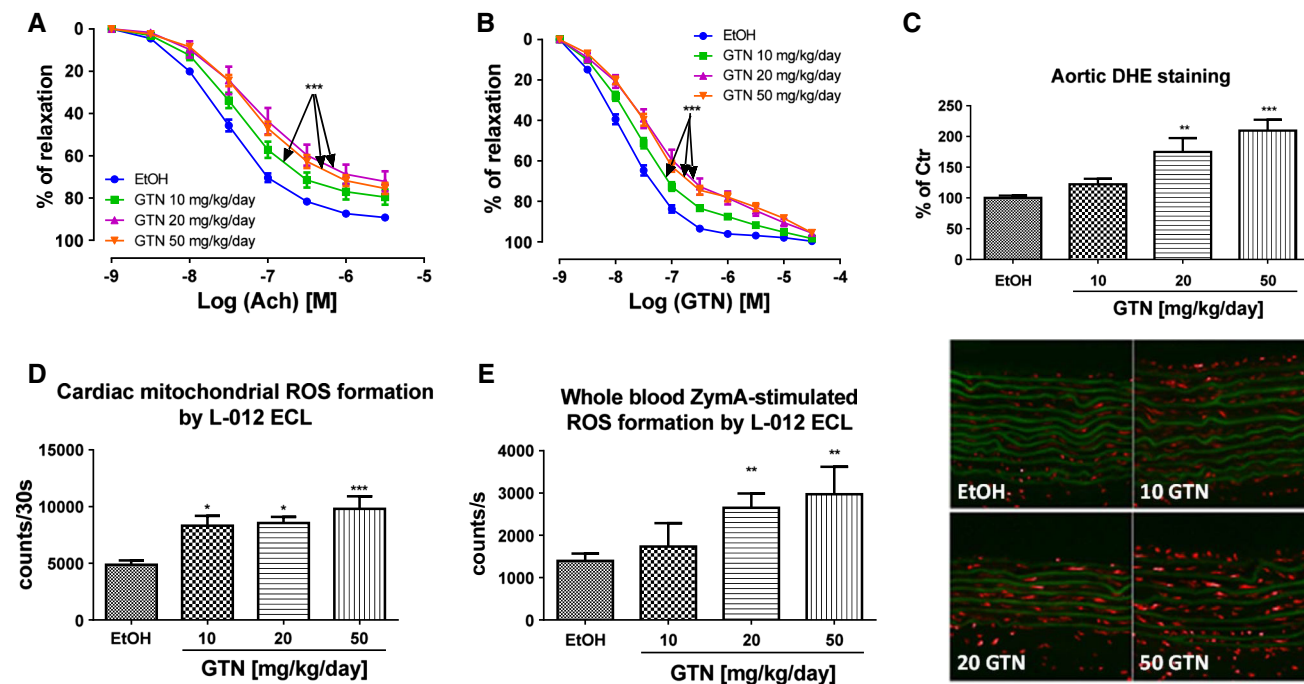
Fig. 2 Endothelial dysfunction, nitrate tolerance and nitro-oxidative stress parameters in GTN-treated Wistar rats. **a** Results of the isometric tension recordings for the endothelium-dependent aortic relaxation, as a read-out for the endothelial dysfunction. **b** Results of the isometric tension recordings for the endothelium-independent aortic relaxation, as a read-out for nitrate tolerance development. **c** DHE-dependent oxidative fluorescence microtopography in cryo-preserved aortic segments as a read-out for vascular RONS formation. Representative images are shown below the densitometric quantification. *Red fluorescence* indicates RONS formation, *green fluorescence* indicates autofluorescence of the basal laminae. **d** Measurement of RONS formation in cardiac mitochondria by L-012-enhanced chemiluminescence. **e** Evaluation of whole blood nitro-oxidative stress, by quantification of the white blood cell-dependent oxidative burst in response to Zymosan A stimulation. The data are presented as mean value $\pm$ SEM of **a** 5–18; **b** 5–18; **c** 5–25; **d** 5–25; **e** 5–25 experimental animals per group. $*p < 0.05$ vs. EtOH-treated solvent control, $**p < 0.01$ vs EtOH-treated solvent control, $***p < 0.001$ vs EtOH-treated solvent control

Chronic GTN treatment causes DNA damage in the aortic and cardiac tissue of Wistar rats

Induction of nitrate tolerance by prolonged GTN treatment was associated with a significant increase in 8-oxo-G and O^6-me-G levels in aorta and heart as measured by dot blot analysis, although no clear dose dependency was observed in all assays (Fig. 3a, b). Increased 8-oxo-G and O^6-me-G levels were also detected by immuno-histochemistry in the aorta and heart of GTN-treated rats throughout the transversal tissue sections (Fig. 3c, d).

Chronic GTN treatment causes apoptosis

Several markers of apoptosis were elevated in tissues from nitrate tolerant rats. Cleavage of caspase-3 is an essential step in the apoptotic cell death pathway and cleaved caspase-3 was increased significantly in the heart in a GTN dose-dependent manner (Fig. 4a). Next, fractin was detected as caspase-specific cleavage product of actin and was shown to dose-dependently increase in cardiac tissue after GTN treatment (Fig. 4b).

Upon activation of apoptotic pathways, cleavage of the genomic DNA takes place, which either leads to low molecular weight DNA fragments or single strand breaks in the high molecular weight DNA fraction. The cell death detection assay (CDD) can be used to quantify the fragmentation of DNA by labeling the free 3′-OH termini with modified nucleotides through an enzymatic reaction (TUNEL). The CDD assay confirmed increased apoptosis in the aorta of GTN-treated rats (Fig. 4c). Finally, we analyzed the levels of p53 tumor suppressor protein, which is known to be activated by genotoxic stress. In line with the observed GTN-dependent induction of DNA damage, p53 levels strongly increased corroborating that high dose GTN therapy is genotoxic (Fig. 4d). The decrease in γH2AX levels in the aorta of GTN-treated rats might be explained by an increased DNA repair activity (Fig. 4d).

Effects of nitrate-free interval on vascular function, oxidative stress and DNA damage

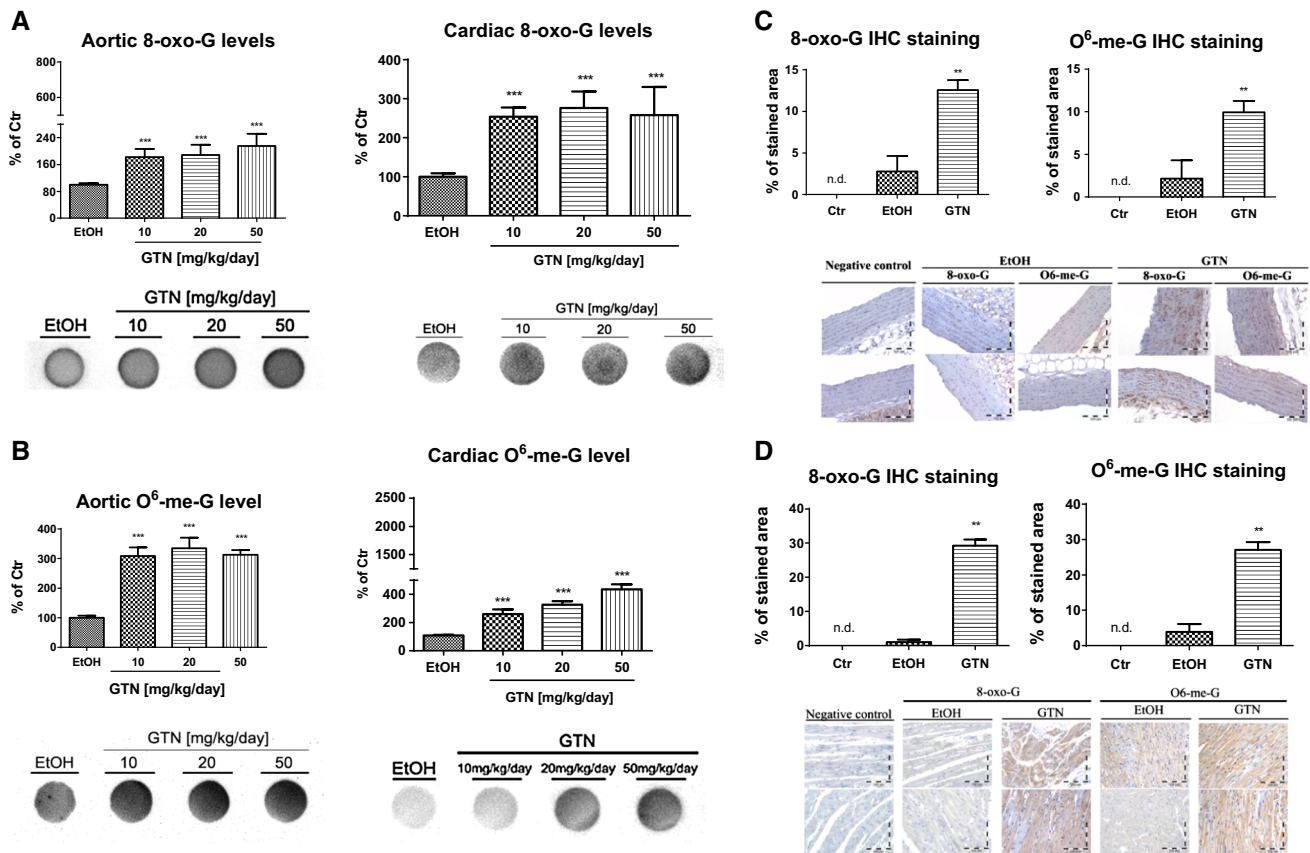High dose GTN treatment for 3.5 days resulted in an impaired aortic response to either ACh or GTN, confirming

Fig. 3 Oxidative and alkylating DNA modifications in GTN-treated Wistar rats. **a** Aortic and cardiac levels of 8-oxo-G after 3.5 days of GTN administration (10, 20 and 50 mg/kg/day) to Wistar rats. Representative dot blots are shown below the densitometric quantification. **b** Aortic and cardiac levels of O^6-me-G in response to increasing GTN doses. Representative dot blots are shown below the densitometric quantification. **c** Aortic levels of 8-oxo-G and O^6-me-G, measured by immuno-histochemistry in samples of solvent- or GTN (50 mg/kg/day)-treated rats. **d** Cardiac levels of 8-oxo-G and O^6-me-G, measured by immuno-histochemistry in samples of solvent- (EtOH)- or GTN (50 mg/kg/day)-treated rats. Representative images are shown below the densitometric quantification. Samples, devoid of the primary antibody treatment, were used as negative controls for IHC measurements. Immuno-histochemical stainings of aortic and cardiac tissue for 8-oxo-G at 100-fold magnification are shown in suppl. Fig. S6. The data are presented as mean value ± SEM of **a** 5–18; **b** 5–18; **c** 6; **d** 6 experimental animals per group. $**p < 0.01$ vs EtOH as solvent control, $***p < 0.001$ vs EtOH solvent control

the development of endothelial dysfunction and nitrate tolerance in the animals (Fig. 5a, b). Levels of vascular ROS, whole blood RONS and cardiac mitochondrial RONS were elevated in the GTN-treated group (Fig. 5c–e). A significant increase in Hb-NO levels in the GTN (high dose) treated animals was observed (Fig. 5f). Increased DNA damage and nitro-oxidative stress in response to GTN therapy was confirmed by immuno-histochemical detection of 8-oxo-G and O^6-me-G adducts as well as 3NT-positive proteins in the rat aorta (Fig. 5g). Importantly, nitrate tolerance, vascular and cardiac mitochondrial oxidative stress as well as nitrosative stress (Hb-NO) were transient and disappeared upon cessation of GTN therapy for 3.5 days (Fig. 5). In contrast, increased levels of 8-oxo-G, O^6-me-G and 3NT were persistent and showed correlation with the partially impaired endothelial function and still increased whole blood (leukocyte-dependent)

oxidative burst in GTN rats after the nitrate-free interval (Fig. 5). Also p53 was still upregulated (by trend) in the aorta of GTN-treated rats after the nitrate-free interval (suppl. Fig. S5).

Nitrate tolerance parameters in MGMT$^{-/-}$ mice

Assessment of the vascular function of isolated aortic ring segments by ACh or GTN concentration-relaxation curves revealed a differential effect of GTN therapy on endothelial function, being more pronounced in MGMT$^{-/-}$ mice (Fig. 6a) but a similar degree of nitrate tolerance in control and MGMT$^{-/-}$ mice upon treatment with GTN for 3.5 days (Fig. 6b). Despite this lack of functional consequence of DNA repair deficiency, the levels of O^6-me-G were increased in the untreated and GTN-treated MGMT$^{-/-}$ group (Fig. 6c, d). In addition, vascular
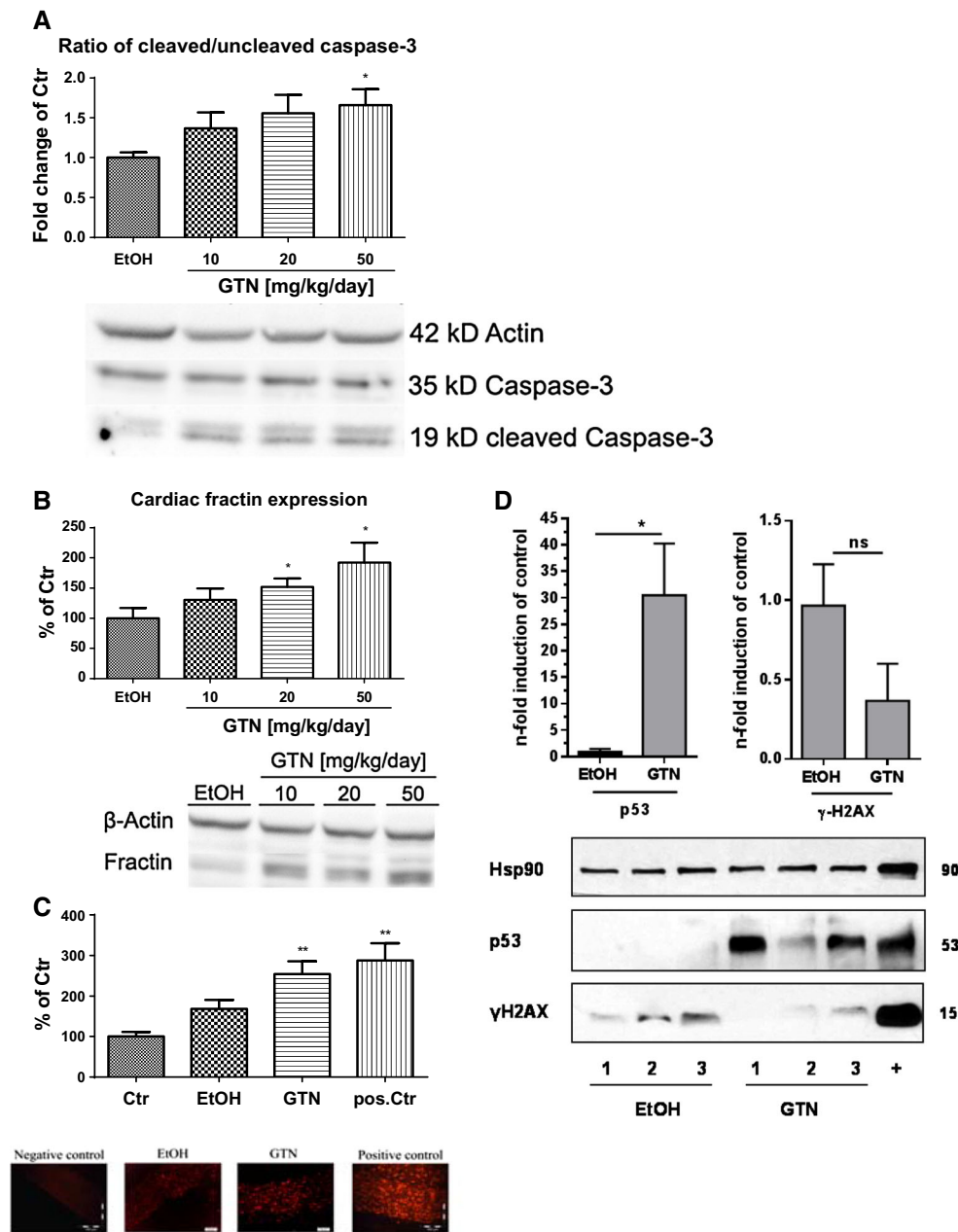
Fig. 4 Increased apoptosis in cardiac and aortic tissue from nitrate tolerant animals. **a** Western blot analysis for cardiac protein expression levels of cleaved caspase-3 as read-out for apoptosis in response to increasing concentrations of GTN. Original Western blots are shown below the densitometric quantification. **b** Western blot results for the cardiac fractin levels in response to increasing concentrations of GTN. Representative blots are shown below the densitometric quantification. **c** Results of the in situ Cell Death Detection kit for quantification of apoptotic endpoints with the help of TUNEL hybridization. Measurement was performed in samples of solvent- or GTN (50 mg/kg/day)-treated rats. As a positive control treatment with DNase I (1500 U/ml) was used. As a negative control,

addition of TUNEL reagent was avoided. Representative images are shown below the densitometric quantification. **d** Western blot analysis for aortic protein expression levels of p53 and γH2AX as read-out for DNA damage response to in vivo GTN treatment (50 mg/kg/day). Original Western blots are shown below the densitometric quantification. As positive control, liver tissue homogenate was used, which was obtained from mice treated with the alkylating agent azoxymethane. The densitometry data are presented as mean value ± SEM of a 3–5; **b** 3–5; **c** 6; 3 **d** experimental animals per group. $*p < 0.05$ vs. EtOH-treated solvent control, $**p < 0.01$ vs EtOH-treated solvent control, $***p < 0.001$ vs EtOH-treated solvent control

oxidative stress showed a more pronounced increase in GTN-treated MGMT$^{-/-}$ mice as compared to controls (Fig. 6e). These findings imply that the direct effect of

prolonged GTN therapy on vascular function and the development of nitrate tolerance are not affected by GTN-induced DNA damage, but the overall nitrate-dependent
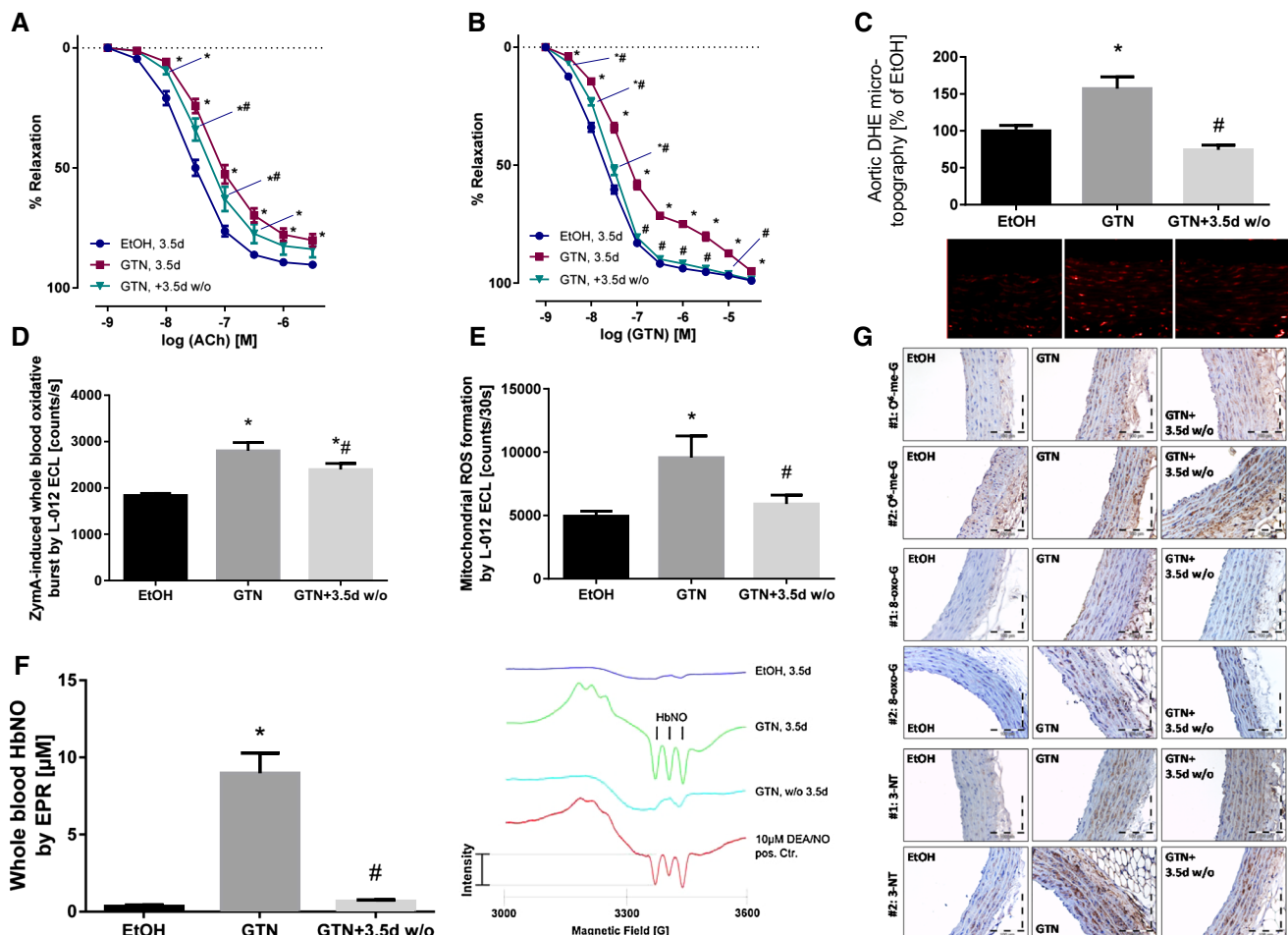
Fig. 5 Impact of 3.5 days of nitrate-free interval (GTN + 3.5 days w/o) on endothelial dysfunction, nitrate tolerance, oxidative stress, DNA damage and 3-nitrotyrosine-positive proteins in response to 3.5 days of continuous GTN (50 mg/kg/day) treatment. **a** Results of the isometric tension recordings for the endothelium-dependent aortic relaxation, as a read-out for the endothelial dysfunction. **b** Results of the isometric tension recordings for the endothelium-independent aortic relaxation, as a read-out for nitrate tolerance development. **c** DHE-dependent oxidative fluorescence microtopography in cryo-preserved aortic segments as a read-out for vascular RONS formation. Representative images are shown below the densitometric quantification. *Red fluorescence* indicates RONS formation. **d** Evaluation of whole blood oxidative burst in response to Zymosan A stimulation. **e** Measurement of RONS formation in cardiac mitochondria by L-012-enhanced chemiluminescence. **f** Determination of whole blood nitrosyl-iron hemoglobin (Hb-NO) levels by EPR as a read-out of GTN-induced nitrosative stress. The original spectra show the presence of the Hb-NO triplet signal in whole blood of GTN-treated rats or DEA/NO-treated whole blood (positive control). **g** Immuno-histochemical data on GTN-mediated DNA damage (O^6-me-G and 8-oxo-G) and the long-term nitro-oxidative stress marker 3-nitrotyrosine-positive proteins. Immuno-histochemical stainings at 100-fold magnification are shown in suppl. Fig. S7. The data are presented as mean value $\pm$ SEM of 8 (EtOH) or 4 (GTN, GTN + 3.5 days w/o) rats (**a–f**); 2 representative images per group are shown out of 4–8 rats per group. *$p < 0.05$ vs. EtOH-treated solvent control, #$p < 0.05$ vs. GTN-treated group

pathogenesis (including cross-tolerance to ACh) seems to be aggravated in MGMT deficient mice, which might contribute to the long-term adverse effects of GTN therapy.

Discussion

In this study, we investigated the molecular mechanisms that contribute to the pathogenesis of nitrate tolerance, a serious side effect of organic nitrate (especially GTN) therapy. Until now, very little attention has been paid to the impact of DNA damage in nitrate tolerance and its potential mutagenic and cytotoxic effects. It was previously demonstrated that organic nitrates increase the level of micronuclei, which reflect chromosomal damage [2]; however, mechanistic insights were not provided. We here focused on previously described DNA damage-associated cell death by apoptosis [51]. We demonstrate the formation of the pre-mutagenic DNA lesions 8-oxo-G and O^6-me-G as well as apoptotic effects upon GTN treatment of cultured cells and in an in vivo setting in animals.
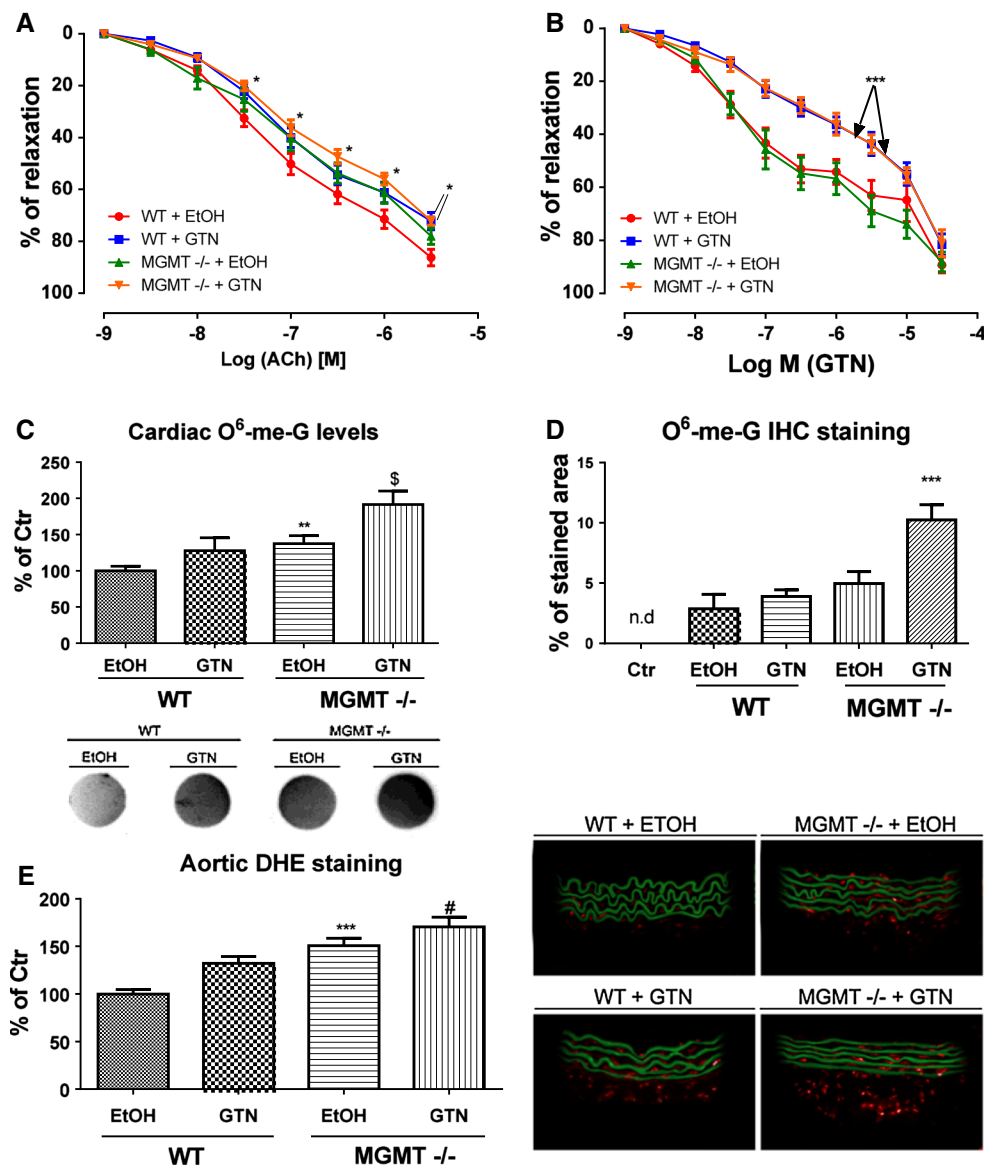
Fig. 6 Comparison of GTN (30 mg/kg/day) effects in MGMT$^{-/-}$ and C57BL/6 mice. **a** Isometric tension recordings of the endothelium-dependent relaxation (ACh response) as a confirmation of nitrate tolerance development. **b** Isometric tension recordings of the endothelium-independent relaxation (GTN response) as a confirmation of nitrate tolerance development. **c** Immuno-dot blot analysis for cardiac levels of O^6-me-G. Representative dot blot is shown below the densitometric quantification. **d** Immuno-histochemical evaluation of the O^6-me-G levels in aorta. Representative images are shown in suppl. Fig. S8. Samples, devoid of the primary antibody treatment, were used as negative controls for IHC quantification. **e** DHE-dependent oxidative fluorescence microtopography in cryo-preserved aortic segments as a read-out for vascular RONS formation. Representative images are shown below the densitometric quantification. *Red fluorescence* indicates RONS formation, *green fluorescence* indicates auto fluorescence of the basal laminae. The data are presented as mean value ± SEM of **a** 9–11; **b** 10–11; **c** 10–11; **d** 6; **e** 10–11 experimental animals per group.*$p < 0.05$ vs. WT EtOH-treated solvent control, **$p < 0.01$ vs WT EtOH-treated solvent control, ***$p < 0.001$ vs WT EtOH-treated solvent control, #$p < 0.01$ vs WT GTN-treated animal, $$p < 0.05$ vs WT GTN-treated animal

In cell culture experiments, using cultured immortal hybridoma cell line EA.hy 926 that shares some key features with human endothelial cells, we observed DNA damage following 48 h incubation with GTN. We demonstrate an elevation of the DNA damage markers, 8-oxo-G and O^6-me-G, and also show an increase in DNA strand breaks. In agreement with this finding, GTN treatment activated the DNA damage response, as revealed by increased levels of p53 and γH2AX. These findings extend previous reports showing that nitric oxide, at least at higher concentrations, has a DNA damaging potential (e.g., through the formation of nitrosamines that are able to alkylate DNA bases or via direct oxidation reaction with the nucleic acid [34]), confers mutagenic effects and

triggers apoptotic pathways [18]. It is also important to note that the highest GTN concentration yielded pronounced cell death, supporting our further observation of increased apoptosis rates induced by the organic nitrate. Other nitric oxide releasing compounds (e.g., SIN-1) also possess DNA damaging properties as previously shown by significant induction of DNA strand breaks in isolated rat islets by the Comet assay [23]. The DNA damaging spectrum of redox active compounds in general and ˙NO releasing compounds in particular is not limited to the direct effects on the nucleic acids, but may also affect the DNA repair machinery [36, 37]. Intriguingly, it has been shown that the DNA repair protein MGMT, which is responsible for the removal of O^6-me-G lesions, is inactivated by ˙NO, leading to its ubiquitin-mediated degradation [33]. In support of these findings, deficiency of S-nitrosoglutathione reductase, which governs cellular protein S-nitrosylation, resulted in S-nitrosylation and subsequent degradation of MGMT under inflammatory conditions in vivo [59]. Thus, long-term medication with organic nitrates reduces MGMT protein levels and thereby may predispose patients to the cytotoxic and pre-mutagenic effects of alkylating agents that are found ubiquitously in food, tobacco and environment [16]. However, the high concentrations used in our cell culture studies represent a limitation of the present study since they are clearly far above the concentration range that can be achieved in rodents and patients [26]. In addition, there is ongoing discussion on the application of the Comet assay, which can be evaluated by DNA migration (tail moment) [54] or by the tail intensity (used in the present study), which both are considered reliable Comet assay parameters for estimation of genotoxicity [56].

With the model of GTN-induced nitrate tolerance in rats we show that the concept of nitrosative/oxidative stress-induced DNA damage also holds true for in vivo conditions and accordingly might have some impact in the clinical setting as well [2]. Nitrate tolerance was clearly correlated with increased cardiovascular nitro-oxidative stress in a GTN dose-dependent fashion and GTN treatment induced a nitrosative milieu, all of which is known to contribute to a higher burden of oxidative/nitrosative DNA damage and strand breaks. Increased formation of 8-oxo-G and O^6-me-G in the DNA upon prolonged treatment with GTN was confirmed in the aorta and heart of rats by two independent methodologies. These DNA lesions are highly mutagenic and their detection in rats treated with GTN at least warrants caution for the clinical use of this drug. In human embryonic kidney cells (HEK 293T) the induction of 8-oxo-G lesions was correlated with highly mutagenic GC–AT transversions [57]. GC–AT transversions are point mutations that may lead to the synthesis of abnormal/dysfunctional proteins. The same is true for O^6-me-G, which is a highly pre-mutagenic DNA lesion that mispairs with thymine, resulting in GC-TA transition mutations [21]. These mutations are frequently found in the Kras oncogene thus contributing to cancer formation (e.g., colon cancer, [16]). In addition, the mitochondrial bioactivation of GTN also implies increased mitochondrial DNA damage, which largely affects myocardial blood flow and its link to metabolism, as previously shown in a model of metabolic syndrome [24]. Circulating mitochondrial DNA (e.g., upon myocardial infarction) may act as a danger signal leading to NF-κB dependent inflammation and cell death of cardiomyocytes [4].

Besides the potential mutagenic effects, we also demonstrate that GTN-induced damage leads to DNA fragmentation and cell death by apoptosis. These findings further support the observation that long-term GTN treatment exacerbated post-ischemic myocardial demise and impaired the functional recovery of the post-ischemic heart in a rat model [17]. The recovery of cardiac tissue after myocardial infarction largely depends on the healing process in the infarcted area, and apoptotic (as well as necrotic) cell death pathways play an important role for the prognosis [49]. Pro-apoptotic effects of GTN were also reported for endothelial progenitor cells (EPC) from GTN-treated healthy volunteers [10]. These cells play an important role in the recovery of the myocardium after cardiovascular events [5, 61]. It remains to be seen whether all organic nitrates share this pro-apoptotic potential and whether this is related to the outcome of meta-analyses of clinical trials with more than 4000 patients with coronary artery diseases, demonstrating that chronic therapy with long-acting organic nitrate was associated with decreased life expectancy [28, 44].

In order to elucidate how persistent the adverse effects of GTN therapy are and whether oxidative and alkylation DNA damage correlate with functional parameters, we also tested the effect of cessation of GTN therapy. The effect of nitrate-free interval was previously studied in detail by Münzel et al. in rabbits [41]. Continuous transdermal GTN treatment (0.4 mg/h = 2.13 mg/kg/day) induced severe nitrate tolerance (impaired GTN-dependent relaxation), endothelial dysfunction (impaired ACh-dependent relaxation) and vascular oxidative stress. All parameters were almost normalized to the placebo-treated control level when a 12-h patch-on/patch-off GTN treatment regimen was applied. Despite this quite positive observations in an animal model, nitrate-free intervals of 12 h in patients seem to decrease the anginal threshold during patch-off intervals due to the phenomenon of rebound ischemia [20, 48]. In our rat model with cessation of GTN treatment for 3.5 days we observed complete normalization of GTN response (no nitrate tolerance anymore), systemic nitrosative stress, cardiovascular oxidative stress but persistent

DNA damage and the long-term marker of nitro-oxidative stress, 3-nitrotyrosine in aortic tissue (Fig. 5). Since endothelial dysfunction was also only partially improved by the nitrate-free interval, we postulate that endothelial cells, rather than smooth muscle cells, are more susceptible to RONS-induced DNA damage and cell death, leading to persistent impairment of function.

We used $MGMT^{-/-}$ mice to address the question of whether accumulation of O^6-me-G DNA adducts occurs in GTN-treated animals that are not able to repair the damage and whether this aggravates the degree of nitrate tolerance. We also considered the possibility that O^6-me-G adduct formation only represents a side effect of nitrate therapy without having significant impact on the pathogenesis of drug-induced complications. Published data show so far no severe phenotype and only demonstrate moderate impact of MGMT deficiency on the life span of mice [35], but MGMT gene polymorphisms have been shown to be associated with increased incidence of neck cancer and other tumors [63]. Our data suggest that MGMT deficiency and O^6-me-G accumulation is unlikely to play a key role for the development and aggravation of nitrate tolerance with respect to vascular function in the 4-day treatment setting (Fig. 6b) but there is evidence that it impacts the degree of cross-tolerance (endothelial dysfunction) (Fig. 6a). Better correlation of DNA damage with endothelial dysfunction is also supported by the observations upon a nitrate-free interval: DNA damage was persistent even after 3.5 days of cessation of GTN therapy and endothelial function was still partially impaired, whereas nitrate tolerance was completely absent in these animals (Fig. 5). It remains to be established whether this long-term adverse effect of GTN therapy on endothelial function (potentially involving persistent oxidative stress and DNA damage) provides an explanation for the observed lower daily activity of patients with heart failure and a preserved ejection fraction under ISMN as compared to placebo therapy [50].

Of note, O^6-me-G only represents one out of many deleterious DNA modifications found upon GTN exposure (e.g., 8-oxo-G and single strand breaks) and the sum of the DNA damage might contribute to nitrate tolerance possibly at the functional level. In addition, the 4-day treatment regimen may be too short to confer the full toxicity of GTN-induced DNA damage. Of note, the $MGMT^{-/-}$ mice were more susceptible to the GTN-induced oxidative stress, which is in our opinion the major trigger of the pathogenesis underlying nitrate tolerance and accounts for most of the serious side effects encountered under long-term organic nitrate therapy. In addition, the induction of cancer following chronic GTN therapy of patients is conflicting: the drug has been used clinically for more than a century without alarming increase in cancer incidence and was even suggested as an anti-cancer drug for non-small-cell lung cancer [62]. On the other hand, the anti-cancer effect of GTN was not confirmed by a recent randomized trial including 372 participants [9]. A major limitation of the studies in mice could be based on their higher resistance to GTN-induced nitrate-induced side effects (e.g., endothelial dysfunction) as previously reported [8].

The activation of intrinsic oxidative and nitrosative pathways by GTN may also lead to the highly protective phenomenon of preconditioning [25] and most probably the treatment duration (acute versus long term) will determine whether GTN elicits beneficial or harmful effects. Interestingly, GTN treatment per se did not interfere with cardiac protection afforded by remote ischemic preconditioning in patients undergoing coronary surgery [30]. A critical evaluation of all the relevant experimental and clinical literature to assess whether exogenous NO (NO gas, nitrite, nitrate or NO donors) given at reperfusion can limit infarct size, revealed highly protective effects for most experimental studies whereas the benefit of these interventions in clinical myocardial infarction is unproven [3].

In conclusion, the present study demonstrates that long-term GTN treatment causes DNA damage in the vascular endothelium, including the mutagenic and cytotoxic adduct O^6-me-G, and apoptotic cell death. The findings may be taken to explain the serious side effects of GTN, namely oxidative stress and associated vascular dysfunction frequently observed during chronic GTN therapy.

References

1. Andreassi MG, Botto N, Simi S, Casella M, Manfredi S, Lucarelli M, Venneri L, Biagini A, Picano E (2005) Diabetes and chronic nitrate therapy as co-determinants of somatic DNA damage in patients with coronary artery disease. J Mol Med (Berl) 83:279–286. doi:10.1007/s00109-005-0634-8

2. Andreassi MG, Picano E, Del Ry S, Botto N, Colombo MG, Giannessi D, Lubrano V, Vassalle C, Biagini A (2001) Chronic long-term nitrate therapy: possible cytogenetic effect in humans? Mutagenesis 16:517–521. doi:10.1093/mutage/16.6.517

3. Bice JS, Jones BR, Chamberlain GR, Baxter GF (2016) Nitric oxide treatments as adjuncts to reperfusion in acute myocardial infarction: a systematic review of experimental and clinical studies. Basic Res Cardiol 111:23. doi:10.1007/s00395-016-0540-y

4. Bliksoen M, Mariero LH, Torp MK, Baysa A, Ytrehus K, Haugen F, Seljeflot I, Vaage J, Valen G, Stenslokken KO (2016) Extracellular mtDNA activates NF-kappaB via toll-like receptor 9 and induces cell death in cardiomyocytes. Basic Res Cardiol 111:42. doi:10.1007/s00395-016-0553-6

5. Britten MB, Abolmaali ND, Assmus B, Lehmann R, Honold J, Schmitt J, Vogl TJ, Martin H, Schachinger V, Dimmeler S, Zeiher AM (2003) Infarct remodeling after intracoronary progenitor cell treatment in patients with acute myocardial infarction (TOPCARE-AMI): mechanistic insights from serial contrast-enhanced magnetic resonance imaging. Circulation 108:2212–2218. doi:10.1161/01.CIR.0000095788.78169.AF

6. Daiber A, Oelze M, August M, Wendt M, Sydow K, Wieboldt H, Kleschyov AL, Munzel T (2004) Detection of superoxide and peroxynitrite in model systems and mitochondria by the luminol analogue L-012. Free Radic Res 38:259–269. doi:10.1080/10715760410001659773

7. Daiber A, Oelze M, Coldewey M, Bachschmid M, Wenzel P, Sydow K, Wendt M, Kleschyov AL, Stalleicken D, Ullrich V, Mulsch A, Munzel T (2004) Oxidative stress and mitochondrial aldehyde dehydrogenase activity: a comparison of pentaerythritol tetranitrate with other organic nitrates. Mol Pharmacol 66:1372–1382. doi:10.1124/mol.104.002600

8. Daiber A, Oelze M, Sulyok S, Coldewey M, Schulz E, Treiber N, Hink U, Mulsch A, Scharffetter-Kochanek K, Munzel T (2005) Heterozygous deficiency of manganese superoxide dismutase in mice (Mn-SOD+/−): a novel approach to assess the role of oxidative stress for the development of nitrate tolerance. Mol Pharmacol 68:579–588. doi:10.1124/mol.105.011585

9. Davidson A, Veillard AS, Tognela A, Chan MM, Hughes BG, Boyer M, Briscoe K, Begbie S, Abdi E, Crombie C, Long J, Boyce A, Lewis CR, Varma S, Broad A, Muljadi N, Chinchen S, Espinoza D, Coskinas X, Pavlakis N, Millward M, Stockler MR, Australasian Lung cancer Trials G, Australasian Lung cancer Trials Group A (2015) A phase III randomized trial of adding topical nitroglycerin to first-line chemotherapy for advanced nonsmall-cell lung cancer: the Australasian lung cancer trials group NITRO trial. Ann Oncol 26:2280–2286. doi:10.1093/annonc/mdv373

10. DiFabio JM, Thomas GR, Zucco L, Kuliszewski MA, Bennett BM, Kutryk MJ, Parker JD (2006) Nitroglycerin attenuates human endothelial progenitor cell differentiation, function, and survival. J Pharmacol Exp Ther 318:117–123. doi:10.1124/jpet.106.102129

11. Dörsam B, Wu CF, Efferth T, Kaina B, Fahrer J (2015) The eucalyptus oil ingredient 1,8-cineol induces oxidative DNA damage. Arch Toxicol 89:797–805. doi:10.1007/s00204-014-1281-z

12. Edgell CJ, McDonald CC, Graham JB (1983) Permanent cell line expressing human factor VIII-related antigen established by hybridization. Proc Natl Acad Sci USA 80:3734–3737

13. Esplugues JV, Rocha M, Nunez C, Bosca I, Ibiza S, Herance JR, Ortega A, Serrador JM, D'Ocon P, Victor VM (2006) Complex I dysfunction and tolerance to nitroglycerin: an approach based on mitochondrial-targeted antioxidants. Circ Res 99:1067–1075. doi:10.1161/01.RES.0000250430.62775.99

14. Fahrer J, Frisch J, Nagel G, Kraus A, Dorsam B, Thomas AD, Reissig S, Waisman A, Kaina B (2015) DNA repair by MGMT, but not AAG, causes a threshold in alkylation-induced colorectal carcinogenesis. Carcinogenesis 36:1235–1244. doi:10.1093/carcin/bgv114

15. Fahrer J, Huelsenbeck J, Jaurich H, Dorsam B, Frisan T, Eich M, Roos WP, Kaina B, Fritz G (2014) Cytolethal distending toxin (CDT) is a radiomimetic agent and induces persistent levels of DNA double-strand breaks in human fibroblasts. DNA Repair (Amst) 18:31–43. doi:10.1016/j.dnarep.2014.03.002

16. Fahrer J, Kaina B (2013) O^6-methylguanine-DNA methyltransferase in the defense against N-nitroso compounds and colorectal cancer. Carcinogenesis 34:2435–2442. doi:10.1093/carcin/bgt275

17. Fan Q, Gao F, Zhang L, Christopher TA, Lopez BL, Ma XL (2005) Nitrate tolerance aggravates postischemic myocardial apoptosis and impairs cardiac functional recovery after ischemia. Apoptosis 10:1235–1242. doi:10.1007/s10495-005-1455-5

18. Felley-Bosco E (1998) Role of nitric oxide in genotoxicity: implication for carcinogenesis. Cancer Metastasis Rev 17:25–37. doi:10.1023/A:1005948420548

19. Ferreira JC, Mochly-Rosen D (2012) Nitroglycerin use in myocardial infarction patients. Circ J 76:15–21. doi:10.1253/circj.CJ-11-1133

20. Freedman SB, Daxini BV, Noyce D, Kelly DT (1995) Intermittent transdermal nitrates do not improve ischemia in patients taking beta-blockers or calcium antagonists: potential role of rebound ischemia during the nitrate-free period. J Am Coll Cardiol 25:349–355. doi:10.1016/0735-1097(94)00416-N

21. Fu D, Calvo JA, Samson LD (2012) Balancing repair and tolerance of DNA damage caused by alkylating agents. Nat Rev Cancer 12:104–120. doi:10.1038/nrc3185

22. Glassner BJ, Weeda G, Allan JM, Broekhof JL, Carls NH, Donker I, Engelward BP, Hampson RJ, Hersmus R, Hickman MJ, Roth RB, Warren HB, Wu MM, Hoeijmakers JH, Samson LD (1999) DNA repair methyltransferase (Mgmt) knockout mice are sensitive to the lethal effects of chemotherapeutic alkylating agents. Mutagenesis 14:339–347. doi:10.1093/mutage/14.3.339

23. Green IC, Cunningham JM, Delaney CA, Elphick MR, Mabley JG, Green MH (1994) Effects of cytokines and nitric oxide donors on insulin secretion, cyclic GMP and DNA damage: relation to nitric oxide production. Biochem Soc Trans 22:30–37. doi:10.1042/bst0220030

24. Guarini G, Kiyooka T, Ohanyan V, Pung YF, Marzilli M, Chen YR, Chen CL, Kang PT, Hardwick JP, Kolz CL, Yin L, Wilson GL, Shokolenko I, Dobson JG Jr, Fenton R, Chilian WM (2016) Impaired coronary metabolic dilation in the metabolic syndrome is linked to mitochondrial dysfunction and mitochondrial DNA damage. Basic Res Cardiol 111:29. doi:10.1007/s00395-016-0547-4

25. Heusch G (2001) Nitroglycerin and delayed preconditioning in humans: yet another new mechanism for an old drug? Circulation 103:2876–2878. doi:10.1161/01.CIR.103.24.2876

26. Jabs A, Oelze M, Mikhed Y, Stamm P, Kroller-Schon S, Welschof P, Jansen T, Hausding M, Kopp M, Steven S, Schulz E, Stasch JP, Munzel T, Daiber A (2015) Effect of soluble guanylyl cyclase activator and stimulator therapy on nitroglycerin-induced nitrate tolerance in rats. Vascul Pharmacol 71:181–191. doi:10.1016/j.vph.2015.03.007

27. Janero DR, Bryan NS, Saijo F, Dhawan V, Schwalb DJ, Warren MC, Feelisch M (2004) Differential nitros(yl)ation of blood and

tissue constituents during glyceryl trinitrate biotransformation in vivo. Proc Natl Acad Sci USA 101:16958–16963. doi:10.1073/pnas.0406075101

28. Kanamasa K, Hayashi T, Kimura A, Ikeda A, Ishikawa K (2002) Long-term, continuous treatment with both oral and transdermal nitrates increases cardiac events in healed myocardial infarction patients. Angiology 53:399–408. doi:10.1177/000331970205300405

29. Kiziltepe T, Hideshima T, Ishitsuka K, Ocio EM, Raje N, Catley L, Li CQ, Trudel LJ, Yasui H, Vallet S, Kutok JL, Chauhan D, Mitsiades CS, Saavedra JE, Wogan GN, Keefer LK, Shami PJ, Anderson KC (2007) JS-K, a GST-activated nitric oxide generator, induces DNA double-strand breaks, activates DNA damage response pathways, and induces apoptosis in vitro and in vivo in human multiple myeloma cells. Blood 110:709–718. doi:10.1182/blood-2006-10-052845

30. Kleinbongard P, Thielmann M, Jakob H, Peters J, Heusch G, Kottenberg E (2013) Nitroglycerin does not interfere with protection by remote ischemic preconditioning in patients with surgical coronary revascularization under isoflurane anesthesia. Cardiovasc Drugs Ther 27:359–361. doi:10.1007/s10557-013-6451-3

31. Knorr M, Hausding M, Kroller-Schuhmacher S, Steven S, Oelze M, Heeren T, Scholz A, Gori T, Wenzel P, Schulz E, Daiber A, Munzel T (2011) Nitroglycerin-induced endothelial dysfunction and tolerance involve adverse phosphorylation and S-Glutathionylation of endothelial nitric oxide synthase: beneficial effects of therapy with the AT1 receptor blocker telmisartan. Arterioscler Thromb Vasc Biol 31:2223–2231. doi:10.1161/ATVBAHA.111.232058

32. Kroller-Schon S, Steven S, Kossmann S, Scholz A, Daub S, Oelze M, Xia N, Hausding M, Mikhed Y, Zinssius E, Mader M, Stamm P, Treiber N, Scharffetter-Kochanek K, Li H, Schulz E, Wenzel P, Munzel T, Daiber A (2014) Molecular mechanisms of the crosstalk between mitochondria and NADPH oxidase through reactive oxygen species-studies in white blood cells and in animal models. Antioxid Redox Signal 20:247–266. doi:10.1089/ars.2012.4953

33. Laval F, Wink DA (1994) Inhibition by nitric oxide of the repair protein, O^6-methylguanine-DNA-methyltransferase. Carcinogenesis 15:443–447. doi:10.1093/carcin/15.3.443

34. Liu RH, Hotchkiss JH (1995) Potential genotoxicity of chronically elevated nitric oxide: a review. Mutat Res 339:73–89. doi:10.1016/0165-1110(95)90004-7

35. Meira LB, Calvo JA, Shah D, Klapacz J, Moroski-Erkul CA, Bronson RT, Samson LD (2014) Repair of endogenous DNA base lesions modulate lifespan in mice. DNA Repair (Amst) 21:78–86. doi:10.1016/j.dnarep.2014.05.012

36. Mikhed Y, Daiber A, Steven S (2015) Mitochondrial oxidative stress, mitochondrial DNA damage and their role in age-related vascular dysfunction. Int J Mol Sci 16:15918–15953. doi:10.3390/ijms160715918

37. Mikhed Y, Gorlach A, Knaus UG, Daiber A (2015) Redox regulation of genome stability by effects on gene expression, epigenetic pathways and DNA damage/repair. Redox Biol 5:275–289. doi:10.1016/j.redox.2015.05.008

38. Munzel T, Daiber A, Gori T (2013) More answers to the still unresolved question of nitrate tolerance. Eur Heart J 34:2666–2673. doi:10.1093/eurheartj/eht249

39. Munzel T, Daiber A, Gori T (2011) Nitrate therapy: new aspects concerning molecular action and tolerance. Circulation 123:2132–2144. doi:10.1161/CIRCULATIONAHA.110.981407

40. Munzel T, Li H, Mollnau H, Hink U, Matheis E, Hartmann M, Oelze M, Skatchkov M, Warnholtz A, Duncker L, Meinertz T, Forstermann U (2000) Effects of long-term nitroglycerin treatment on endothelial nitric oxide synthase (NOS III) gene expression, NOS III-mediated superoxide production, and

vascular NO bioavailability. Circ Res 86:E7–E12. doi:10.1161/01.RES.86.1.e7

41. Munzel T, Mollnau H, Hartmann M, Geiger C, Oelze M, Warnholtz A, Yehia AH, Forstermann U, Meinertz T (2000) Effects of a nitrate-free interval on tolerance, vasoconstrictor sensitivity and vascular superoxide production. J Am Coll Cardiol 36:628–634. doi:10.1016/S0735-1097(00)00754-3

42. Munzel T, Sayegh H, Freeman BA, Tarpey MM, Harrison DG (1995) Evidence for enhanced vascular superoxide anion production in nitrate tolerance. A novel mechanism underlying tolerance and cross-tolerance. J Clin Invest 95:187–194. doi:10.1172/JCI117637

43. Munzel T, Wenzel P, Daiber A (2007) Do we still need organic nitrates? J Am Coll Cardiol 49:1296–1298. doi:10.1016/j.jacc.2007.01.007

44. Nakamura Y, Moss AJ, Brown MW, Kinoshita M, Kawai C (1999) Long-term nitrate use may be deleterious in ischemic heart disease: a study using the databases from two large-scale postinfarction studies. Multicenter Myocardial Ischemia Research Group. Am Heart J 138:577–585. doi:10.1016/S0002-8703(99)70163-8

45. Nehls P, Adamkiewicz J, Rajewsky MF (1984) Immuno-slot-blot: a highly sensitive immunoassay for the quantitation of carcinogen-modified nucleosides in DNA. J Cancer Res Clin Oncol 108:23–29. doi:10.1007/BF00390969

46. Oelze M, Daiber A, Brandes RP, Hortmann M, Wenzel P, Hink U, Schulz E, Mollnau H, von Sandersleben A, Kleschyov AL, Mulsch A, Li H, Forstermann U, Munzel T (2006) Nebivolol inhibits superoxide formation by NADPH oxidase and endothelial dysfunction in angiotensin II-treated rats. Hypertension 48:677–684. doi:10.1161/01.HYP.0000239207.82326.29

47. Oelze M, Knorr M, Kroller-Schon S, Kossmann S, Gottschlich A, Rummler R, Schuff A, Daub S, Doppler C, Kleinert H, Gori T, Daiber A, Munzel T (2013) Chronic therapy with isosorbide-5-mononitrate causes endothelial dysfunction, oxidative stress, and a marked increase in vascular endothelin-1 expression. Eur Heart J 34:3206–3216. doi:10.1093/eurheartj/ehs100

48. Parker JD, Parker AB, Farrell B, Parker JO (1995) Intermittent transdermal nitroglycerin therapy. Decreased anginal threshold during the nitrate-free interval. Circulation 91:973–978. doi:10.1161/01.CIR.91.4.973

49. Rassaf T, Weber C, Bernhagen J (2014) Macrophage migration inhibitory factor in myocardial ischaemia/reperfusion injury. Cardiovasc Res 102:321–328. doi:10.1093/cvr/cvu071

50. Redfield MM, Anstrom KJ, Levine JA, Koepp GA, Borlaug BA, Chen HH, LeWinter MM, Joseph SM, Shah SJ, Semigran MJ, Felker GM, Cole RT, Reeves GR, Tedford RJ, Tang WH, McNulty SE, Velazquez EJ, Shah MR, Braunwald E, Network NHFCR (2015) Isosorbide mononitrate in heart failure with preserved ejection fraction. N Engl J Med 373:2314–2324. doi:10.1056/NEJMoa1510774

51. Roos WP, Kaina B (2013) DNA damage-induced cell death: from specific DNA lesions to the DNA damage response and apoptosis. Cancer Lett 332:237–248. doi:10.1016/j.canlet.2012.01.007

52. Schuhmacher S, Foretz M, Knorr M, Jansen T, Hortmann M, Wenzel P, Oelze M, Kleschyov AL, Daiber A, Keaney JF Jr, Wegener G, Lackner K, Munzel T, Viollet B, Schulz E (2011) alpha1AMP-activated protein kinase preserves endothelial function during chronic angiotensin II treatment by limiting Nox2 upregulation. Arterioscler Thromb Vasc Biol 31:560–566. doi:10.1161/ATVBAHA.110.219543

53. Schuhmacher S, Schulz E, Oelze M, Konig A, Roegler C, Lange K, Sydow L, Kawamoto T, Wenzel P, Munzel T, Lehmann J, Daiber A (2009) A new class of organic nitrates: investigations on bioactivation, tolerance and cross-tolerance phenomena. Br J Pharmacol 158:510–520. doi:10.1111/j.1476-5381.2009.00303.x

54. Speit G, Schutz P, Bonzheim I, Trenz K, Hoffmann H (2004) Sensitivity of the FPG protein towards alkylation damage in the comet assay. Toxicol Lett 146:151–158. doi:10.1016/j.toxlet.2003.09.010

55. Spieker LE, Flammer AJ, Luscher TF (2006) The vascular endothelium in hypertension. Handb Exp Pharmacol. doi:10.1007/3-540-36028-X

56. Sunjog K, Kolarevic S, Heberger K, Gacic Z, Knezevic-Vukcevic J, Vukovic-Gacic B, Lenhardt M (2013) Comparison of comet assay parameters for estimation of genotoxicity by sum of ranking differences. Anal Bioanal Chem 405:4879–4885. doi:10.1007/s00216-013-6909-y

57. Suzuki T, Harashima H, Kamiya H (2010) Effects of base excision repair proteins on mutagenesis by 8-oxo-7,8-dihydroguanine (8-hydroxyguanine) paired with cytosine and adenine. DNA Repair (Amst) 9:542–550. doi:10.1016/j.dnarep.2010.02.004

58. Sydow K, Daiber A, Oelze M, Chen Z, August M, Wendt M, Ullrich V, Mulsch A, Schulz E, Keaney JF Jr, Stamler JS, Munzel T (2004) Central role of mitochondrial aldehyde dehydrogenase and reactive oxygen species in nitroglycerin tolerance and cross-tolerance. J Clin Invest 113:482–489. doi:10.1172/JCI19267

59. Wei W, Li B, Hanes MA, Kakar S, Chen X, Liu L (2010) S-nitrosylation from GSNOR deficiency impairs DNA repair and promotes hepatocarcinogenesis. Sci Transl Med 2:19. doi:10.1126/scitranslmed.3000328

60. Wenzel P, Mollnau H, Oelze M, Schulz E, Wickramanayake JM, Muller J, Schuhmacher S, Hortmann M, Baldus S, Gori T, Brandes RP, Munzel T, Daiber A (2008) First evidence for a crosstalk between mitochondrial and NADPH oxidase-derived reactive oxygen species in nitroglycerin-triggered vascular dysfunction. Antioxid Redox Signal 10:1435–1447. doi:10.1089/ars.2007.1969

61. Werner C, Bohm M, Friedrich EB (2008) Progenitor cell therapy and myocardial infarction: the importance of microvascular function. Nat Clin Pract Cardiovasc Med 5:78–79. doi:10.1038/ncpcardio1058

62. Yasuda H, Yamaya M, Nakayama K, Sasaki T, Ebihara S, Kanda A, Asada M, Inoue D, Suzuki T, Okazaki T, Takahashi H, Yoshida M, Kaneta T, Ishizawa K, Yamanda S, Tomita N, Yamasaki M, Kikuchi A, Kubo H, Sasaki H (2006) Randomized phase II trial comparing nitroglycerin plus vinorelbine and cisplatin with vinorelbine and cisplatin alone in previously untreated stage IIIB/IV non-small-cell lung cancer. J Clin Oncol 24:688–694. doi:10.1200/JCO.2005.04.0436

63. Zhang Z, Wang L, Wei S, Liu Z, Wang LE, Sturgis EM, Wei Q (2010) Polymorphisms of the DNA repair gene MGMT and risk and progression of head and neck cancer. DNA Repair (Amst) 9:558–566. doi:10.1016/j.dnarep.2010.02.006